Acta Oceanol. Sin., 2020, Vol. 39, No. 9, P. 125–132
https://doi.org/10.1007/s13131-020-1652-7
http://www.hyxb.org.cn
E-mail: hyxbe@263.net

Under-ice ambient noise in the Arctic Ocean: observations at the long-term ice station

Xiao Han[1, 2, 3], Jingwei Yin[1, 2, 3]*, Yanming Yang[4], Hongtao Wen[4], Longxiang Guo[1, 2, 3]

[1] Acoustic Science and Technology Laboratory, Harbin Engineering University, Harbin 150001, China

[2] Key Laboratory of Marine Information Acquisition and Security (Harbin Engineering University), Ministry of Industry and Information Technology, Harbin 150001, China

[3] College of Underwater Acoustic Engineering, Harbin Engineering University, Harbin 150001, China

[4] Laboratory of Ocean Acoustic and Remote Sensing, Third Institute of Oceanography, Ministry of Natural Resources, Xiamen 361005, China

Received 14 December 2019; accepted 24 March 2020

Abstract

Under-ice ambient noise in the Arctic Ocean is studied using the data recorded by autonomous hydrophones at the long-term ice station during the 9th Chinese National Arctic Research Expedition. Time-frequency analysis of two 7-s-long ice-induced noise samples shows that both ice collision and ice breaking noise have many outliers in the time-domain (impulsive characteristic) and abundant frequency components in the frequency-domain. Ice collision noise lasts for several seconds while the duration of ice breaking noise is much shorter (i.e., less than tens of milliseconds). Gaussian distribution and symmetric alpha stable (sαs) distribution are used in this paper to fit the impulsive under-ice noise. The sαs distribution can achieve better performance as it can track the heavy tails of impulsive noise while Gaussian distribution fails. This paper also analyzes the meteorological variables during the under-ice noise observation experiment and deduces that the impulsive ambient noise was caused by the combined force of high wind speed and increasing atmosphere temperature on the ice canopy. The Pearson correlation coefficients between long-term power spectral density variations of under-ice ambient noise and meteorological variables are also studied in this paper.

Key words: long-term ice station, under-ice ambient noise, time-frequency analysis, power spectral density variations, meteorological variables

Citation: Han Xiao, Yin Jingwei, Yang Yanming, Wen Hongtao, Guo Longxiang. 2020. Under-ice ambient noise in the Arctic Ocean: observations at the long-term ice station. Acta Oceanologica Sinica, 39(9): 125–132, doi: 10.1007/s13131-020-1652-7

1 Introduction

Ocean ambient noise is one of the most important research topics in underwater acoustic as it can greatly affect the performance of underwater sonars (i.e., communication and detection). Therefore, a large amount of literature has been reported on ocean ambient noise in order to understand its temporal, spatial and frequency characteristics (Audoly et al., 2017; Brooker and Humphrey, 2016; Bittencourt et al., 2017; Da et al., 2014; Lin et al., 2005; Yang et al., 2018). In most oceans on the earth, ambient noise is mainly caused by thermal movement of seawater, hydrodynamic force (i.e., waves, tides, and currents), ocean biology (i.e., dolphins and whales), and man-made activity (i.e., shipping and exploration). However, the ocean ambient noise in the Arctic Ocean can also be produced by the combination of thermal, wind, and current stresses on the ice canopy in addition to the above sources. Ice events due to ice cracking, ice fracturing, ice breaking, ice shearing, ice ridging, ice collision, ice melting, and ice drifting can all produce ice-induced noise (Milne and Ganton, 1964; Ganton and Milne, 1965; Urick, 1984; Carey and Evans, 2011; Roth et al., 2012).

Under-ice ambient noise in the Arctic Ocean has been extensively studied since the end of last century and most of these researches focus on under-ice noise characteristics and the relationship between under-ice noise and meteorological variables. A new method is presented to explain how noise is generated under pack ice by ridging of the pack ice and simulated noise was compared with observations for an experiment conducted during the winter in the Beaufort Sea (Pritchard, 1984). Makris and Dyer (1986) showed that low-frequency ambient noise under pack ice was highly correlated with comprehensive stress caused by wind, current and drift. They then studied low-frequency ambient noise under drifting floes of the marginal ice zone and found that the long-term variations of the noise are strongly related to surface gravity wave forcing (Makris and Dyer, 1991). Under-ice ambient noise in the Beaufort Sea has been studied including its seasonal characteristics, seasonal space and time scales, and seasonal relationship to sea ice (Lewis and Denner, 1987, 1988a). Lewis also analyzed higher frequency (1 000 Hz) ambient noise in the Arctic Ocean (Lewis and Denner, 1988b) and the relationship between Arctic ambient noise and thermally

Foundation item: The National Natural Science Foundation of China under contract Nos 61631008, 61901136 and 51779061; the National Key Research and Development Program of China under contract No. 2018YFC1405904; the Fok Ying-Tong Education Foundation under contract No. 151007; the Opening Funding of Science and Technology on Sonar Laboratory under contract No. 6142109KF201802; the Innovation Special Zone of National Defense Science and Technology.
*Corresponding author, E-mail: yinjingwei@hrbeu.edu.cn

induced fracturing of the ice pack (Lewis, 1994). Greening (1994) found that spatial distribution of ice cracking was consistent with a uniform distribution and source levels were usually from 110 dB re $\mu Pa^2/Hz$ to 180 dB re $\mu Pa^2/Hz$.

The research of ambient noise in the Arctic Ocean is not so active from the end of last century to almost 2010 and only few literature reported on this topic during this period of time. Johannessen et al. (2003) demonstrated that acoustic hotspots along the ice-edge region are due to mesoscale eddy currents interacting with the broken-up ice floes in the Greenland and Barents Seas' marginal ice zone. Recently, ambient noise in the Arctic Ocean has re-attracted attention of researchers. Roth et al. (2012) analyzed the mean monthly spectrum levels of ambient noise on the Chukchi Sea continental slope from 2006–2009 and found that months with open-water had the highest noise levels and months with both ice cover and low wind speeds had the lowest noise levels. Kinda et al. (2013) studied under-ice ambient noise in Eastern Beaufort Sea, Canadian Arctic, and its relation to environmental forcing and showed that under-ice ambient noise had consistent correlations with large-scale regional ice drift, wind speed, and measured currents in upper water column. The noise transients in the under-ice ambient noise were further analyzed and sorted into three categories (Kinda et al., 2015). The directionality of the ambient noise field in an Arctic, glacial bay was measured and the results showed that different classes of source radiate noise in distinct spectral bands and were spatially diverse (Deane et al., 2014). Ambient noise in the eastern Arctic was studied using a drifting vertical hydrophone array and showed that the main sources of under-ice noise are broadband and tonal ice noises, bowhead whale calling, seismic airgun surveys, and earthquake *T* phases (Ozanich et al., 2017).

Although under-ice ambient noise in the Arctic Ocean has been extensively studied, most of the existing work analyzes the characteristics of large time scale noise and its relationship with the environment variables and there is little work reporting the characteristics of sea ice-induced impulsive ambient noise in detail. In this paper, we will show the time, frequency and amplitude distribution characteristics of two sea ice-induced impulsive ambient noises (ice collision noise and ice breaking noise) which were recorded by autonomous hydrophones at the long-term ice station during the 9th Chinese National Arctic Research Expedition and reveal the relationship between under-ice ambient noise and meteorological variables. The rest of this paper is organized as follows: Section 2 gives the details of the under-ice ambient noise observation experiment; Section 3 shows the analysis results of impulsive ambient noise and its relationship with meteorological variables; and Section 4 summarizes the whole paper.

2 Under-ice ambient noise observation experiment

Under-ice ambient noise observation experiment was conducted at the long-term ice station at 84°09′47.10″N, 167°15′44.38″W (as shown in Fig. 1a) on August 18, 2018 from 01:46 to 18:56 (GMT) during the 9th Chinese National Arctic Research Expedition. Figure 1b shows the ice condition at the edge of the long-term ice station from which one can see many stacked ices which were caused by ice canopy events. A vertical array with eight autonomous hydrophones which were uniformly spaced by 10 m was used to record under-ice ambient noise. Figure 1c shows two hydrophones used in this experiment. Note that the vertical array was deployed very close to the edge of the long-term ice station in order to record more sea ice-induced noise. The data from the hydrophone deployed to 30 m depth is used in this paper. The receiving sensitivity of hydrophones is relatively flat at (-170 ± 2) dB re 1 V μPa^{-1} over the working bandwidth 20 Hz to 20 kHz and the sampling frequency is 50 kHz. From 16:00 to 17:00 (GMT) on August 18 during this experiment, the ice activity near the vertical array was relatively intense and a large crack appeared on the ice canopy at the long-term ice station. Therefore, a few ice collision and ice breaking noises happened to be recorded by the hydrophones.

3 Analysis of under-ice ambient noise

3.1 *The Arctic ice collision noise*

The raw acoustic recordings were converted to instantaneous sound pressure using the analog-to-digital conversion parameters, the gain, and the hydrophone receiving sensitivity calibration. Figure 2 shows a sample of the ice collision noise in time do-

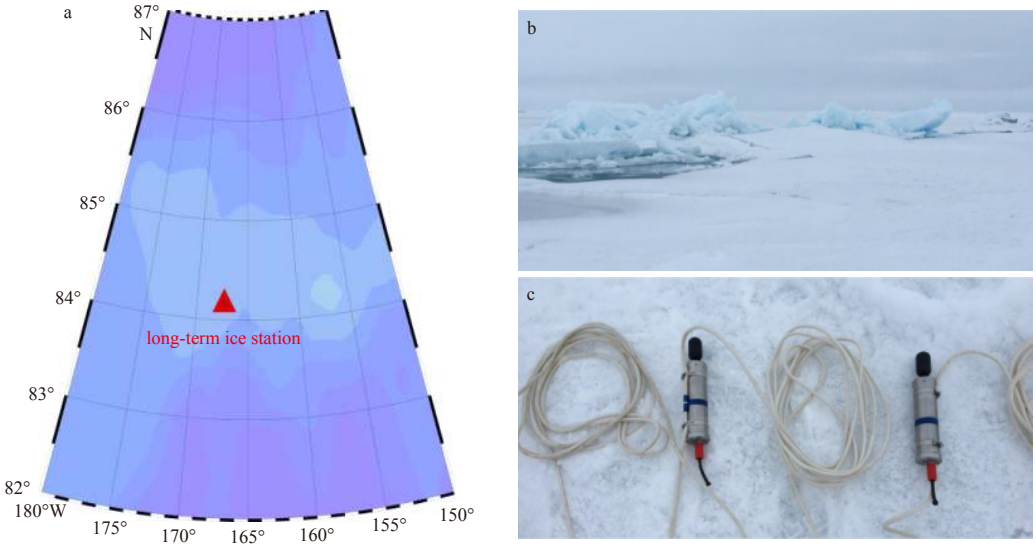

Fig. 1. The under-ice ambient noise observation experiment location of the long-term ice station (a), the ice condition at the edge of the long-term ice station (b), and two hydrophones used in the experiment (c).

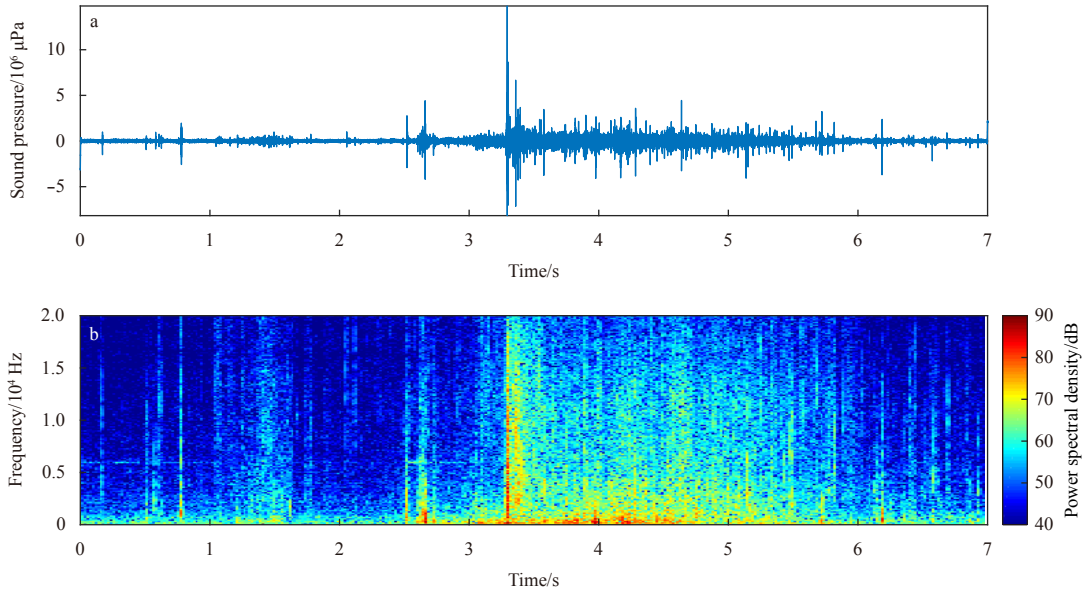

Fig. 2. The time domain waveform of the Arctic ice collision noise recorded by autonomous hydrophone at the long-term ice station during the 9th Chinese National Arctic Research Expedition (a); and the corresponding time-frequency analysis (spectrogram) of the Arctic ice collision noise shown in Fig. 2a (b).

main from which one can clearly see many outliers. The amplitudes of these outliers are much greater than those of normal under-ice ambient noise. It can also be seen from Fig. 2a that the ice collision noise lasts for a few seconds (>3 s). It is reasonable because the collision event between ice canopies was not instantaneous and a lot of ice cracking and squeezing phenomenon happened during this process. One can also calculate the spectrogram of under-ice ambient noise using the "spectrogram" function in MATLAB software. In this paper, the fast Fourier transform point was 2 048, the overlap rate was 50%, and the window function was the default Hamming window of the spectrogram function. Figure 2b is the corresponding time-frequency analysis (spectrogram) of the Arctic ice collision noise shown in Fig. 2a. The Arctic ice collision noise has very abundant frequency components which are from very low frequency to very high frequency. However, most of its energy is concentrated in the lower frequency band (<1 kHz).

We use two distributions (symmetric alpha stable (sαs) distribution and Gaussian distribution) to fit the under-ice ambient noise. sαs distribution is a kind of heavy-tailed distribution and usually used in economics and physics as models of rare, but extreme events (i.e., earthquakes or stock market crashes) (Huang et al., 2013; Shen et al., 2016; Stoyanov et al., 2006). Suppose $\{x_1, x_2, \cdots, x_n\}$ are independent and identically distributed random variables with sαs distribution, then the characteristic function can be given by $\varphi(t) = \mathrm{e}^{-r|t|^{\alpha}}$, where α is characteristic exponent and describes the tail of the distribution. The smaller α is, the more severe the tail of the distribution is. γ is scale parameter and is similar to the variance in Gaussian distribution. This paper uses the method presented by McCulloch (1986) to estimate the two parameters when fitting the amplitude of under-ice ambient noise. Figure 3 shows the probability density function (PDF) curves of amplitude of the Arctic ice collision noise. Note that we use the raw data (the data after analog-to-digital conversion) rather than the converted sound pressure to do the statistical analysis. The red line in Fig. 3 is the fitting result by sαs distribution with the characteristic exponent α=1.22 and the scale parameter γ=529 while the black line is the fitting result by Gaussian distribution with the mean μ=18.7 and the variance δ=1 744. One can easily find from Fig. 3 that sαs distribution can fit better with the experimental data than Gaussian distribution. As well known, sαs distribution degenerates into a Gaussian distribution when α=2. A much smaller characteristic exponent in the fitting result means that this ice collision noise sample is very impulsive. Therefore, algorithms which assume that ambient noise follows Gaussian distribution will suffer severe performance degradation under the ice collision noise environment. Note that we use log-scale for both axes in Fig. 3. By using the log-scale for x-axis, one can easily see how well different distributions fit the real data especially for the outliers. In order to plot the log-scale figures, this paper uses the absolute value of the real data in the statistic. It can also be seen from Fig. 3 that the PDF of the real data has a very heavy tail. sαs distribution also has a heavy tail while Gaussian distribution has a sharp PDF decrease for the large values (i.e., >3 000) which again demonstrates that sαs distribution can fit better for the real data compared with Gaussian distribution.

3.2 *The Arctic ice breaking noise*

Figure 4a shows a sample of the Arctic ice breaking noise in time domain from which one can also see some outliers. Though their amplitudes are much greater than other under-ice ambient noise, they last very short time (i.e., several milliseconds or dozens of milliseconds). It is also reasonable because the ice breaking event happened instantaneously. Figure 4b is the corresponding time-frequency analysis (spectrogram) of the Arctic ice breaking noise shown in Fig. 4a. The Arctic ice breaking noise also has very abundant frequency components which are from very low frequency to very high frequency. However, most of its energy is also concentrated in the lower frequency band (<3 kHz) which is much higher than the ice collision noise. Note that the 12 kHz interference (marked by red circles in Fig. 4) was from the ocean depth measuring sonar on the R/V *Xuelong*.

Figure 5 shows the amplitude statistical characteristics of the Arctic ice breaking noise. Note that we also use the raw data (the

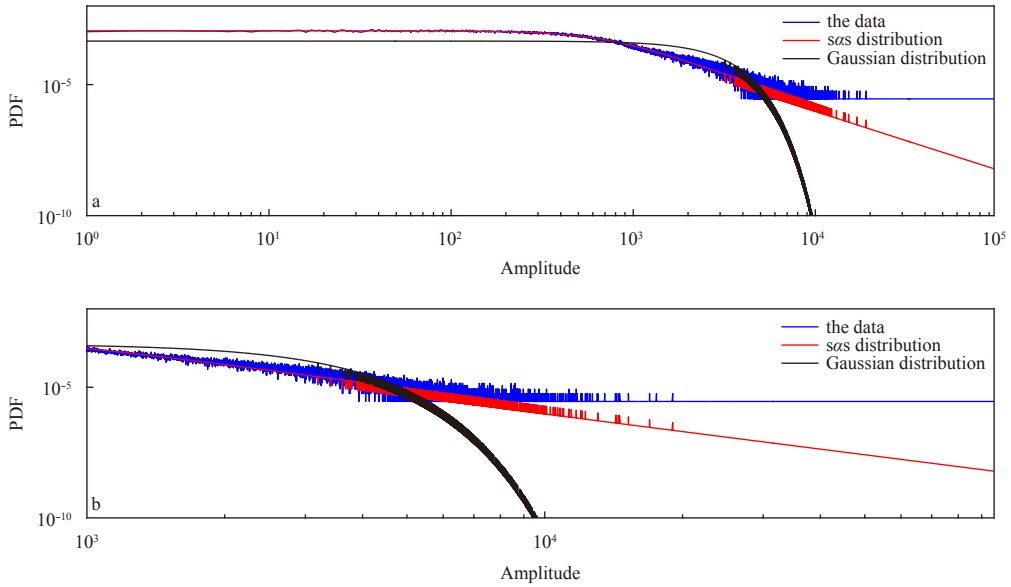

Fig. 3. The statistical characteristics of the Arctic ice collision noise shown in Fig. 2a and the fitting results by two distributions (sαs distribution and Gaussian distribution) (a); and a zoom in Fig. 3a when limiting the amplitude greater than 1 000 (b).

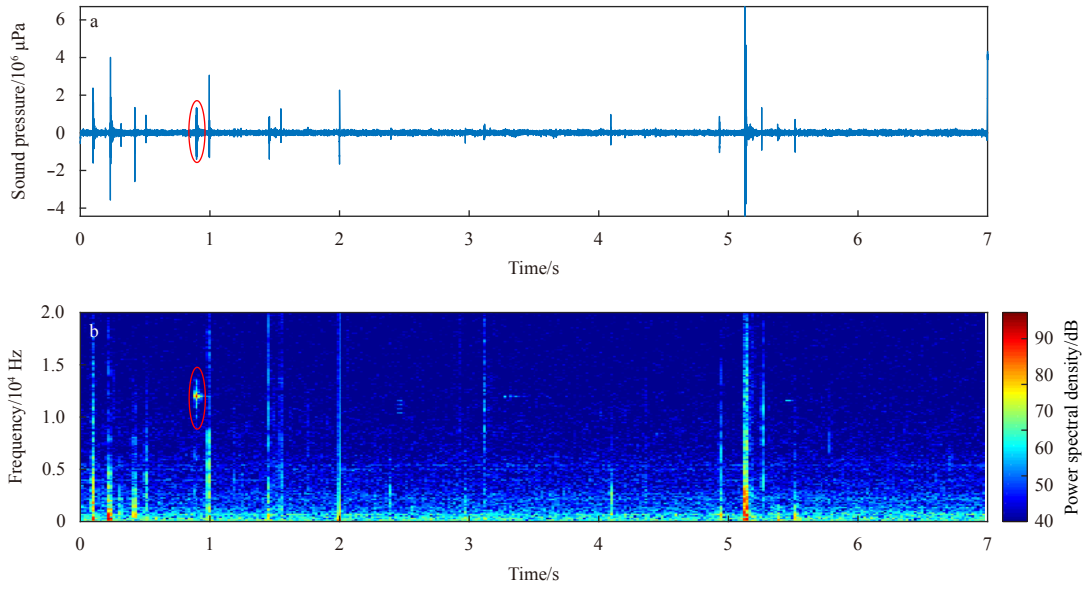

Fig. 4. The time domain waveform of the Arctic ice breaking noise recorded by autonomous hydrophone at the long-term ice station during the 9th Chinese National Arctic Research Expedition (a); and the corresponding time-frequency analysis (spectrogram) of the Arctic ice breaking noise shown in Fig. 4a (b).

data after analog-to-digital conversion) to do the statistical analysis. The red line in Fig. 5 is the fitting result by sαs distribution with the characteristic exponent α=1.91 and the scale parameter γ=262 while the black line is the fitting result by Gaussian distribution with the mean μ=24.6 and the variance δ=779. One can easily find from Fig. 5 that the sαs distribution can fit better with the data than Gaussian distribution. A much larger characteristic exponent in the fitting results means that the ice breaking noise sample is not so impulsive as the ice collision noise sample. It is understandable because though the instantaneous ice breaking activity can produce strong impulsive noises, this phenomenon did not always happen. Actually, it happened rarely with very short duration. Therefore, these occasional ice breaking noises cannot greatly affect the characteristic exponent in terms of long-time statistics. Note that we also use log-scale for both axes in Fig. 5. It can be seen from Fig. 5 that the PDF of Arctic breaking noise also has a heavy tail. sαs distribution can fit well for the outliers while Gaussian distribution has a sharp PDF decrease for the large values (i.e., >2 000).

3.3 *The relationship between under-ice noise and meteorological variables*

Figure 6 shows the meteorological variables including atmosphere temperature and wind speed recorded on August 18 by meteorological stations on the R/V *Xuelong*. As mentioned above, the ice collision and ice breaking noises were recorded

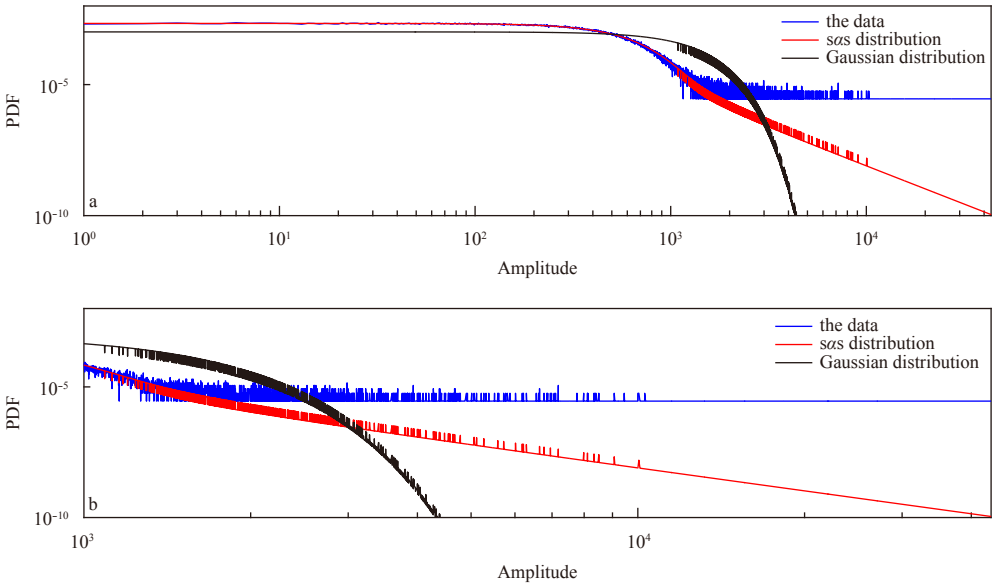

Fig. 5. The statistical characteristics of the Arctic ice breaking noise and the fitting results by two distributions (sαs distribution and Gaussian distribution) (a); and a zoom in Fig. 5a when limiting the amplitude greater than 1 000 (b).

during the period from 16:00 to 17:00 which are marked by two red lines in Fig. 6. This phenomenon demonstrates that the ice canopy was relatively active during this period. Therefore, a natural question will arise why the ice canopy was so active during this period. One may find some clues from the recorded meteorological variables. It can be seen from Fig. 6 that the wind speed increased obviously from 9:00 and got to the maximum value around 16:00. During this period the atmosphere temperature also increased gradually. The increasing wind speed would definitely make the ice canopy move and the increasing atmosphere temperature would accelerate the melting of the ice canopy and make its structure more unstable. Therefore, it is reasonable to make the conclusion that the impulsive ambient noise was caused by the combined force of high wind speed and increasing atmosphere temperature on the ice canopy.

The Pearson correlation coefficients between long-term power spectral density (PSD) variations of under-ice ambient noise and meteorological variables will be analyzed in the following context. Pearson correlation coefficient is a measure of the linear correlation between two variables. Given paired data $\{(x_1, y_1), (x_2, y_2), \cdots, (x_n, y_n)\}$ consisting of n pairs, Pearson correlation coefficient r_{xy} is defined as

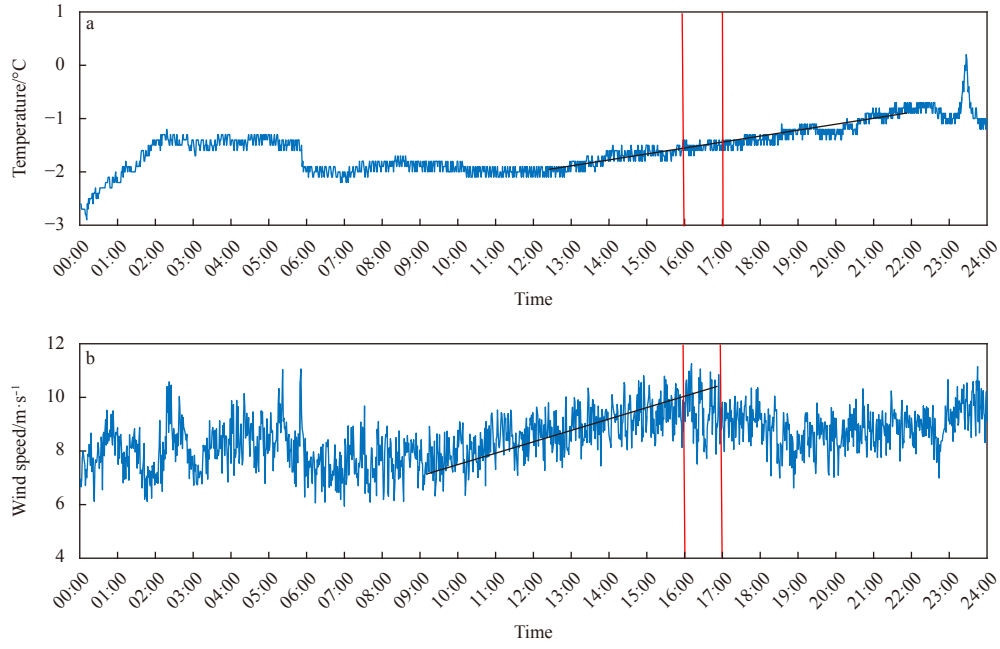

Fig. 6. Atmosphere temperature (a) and wind speed (b), recorded on August 18 by meteorological station on the R/V *Xuelong*. The red lines mark the period when the ice canopy was relatively active. The black lines show the increasing trend of the two meteorological parameters.

$$r_{xy}=\frac{\sum_{i=1}^{n}(x_i-\bar{x})(y_i-\bar{y})}{\sqrt{\sum_{i=1}^{n}(x_i-\bar{x})^2}\sqrt{\sum_{i=1}^{n}(y_i-\bar{y})^2}}, \quad (1)$$

where n is the sample size, x_i and y_i are the individual sample points indexed with i, $\bar{x}=\frac{1}{n}\sum_{i=1}^{n}x_i$ (the sample mean) and analogously for $\bar{y}$.

Note that the first hour and the last hour noise data are excluded in data processing as many scientific researchers were working on the long-term ice station to deploy or recycle their facilities during these periods, producing a lot of noise which may influence the analysis results. The hydrophones autonomously stored ambient noise data every 8 min. A total of 114 segments of 8-min-long noise data were obtained for this under-ice ambient noise observation experiment. Figure 7 shows the meteorological variables that are averaged every 8 min corresponding to the length of each data file. It can be seen from Fig. 7a that the temperature was relatively stable at the beginning of the experiment, but there is a sharp fall around 05:42. The atmosphere temperature fluctuated from 06:42 to 12:42. Then the temperature gradually increased from 12:42. The wind speed also decreased around 05:42 and it gradually increased from 06:42 to 15:42 and then became relatively stable.

Figure 8a shows the PSD variations along with time at 150 Hz, 450 Hz, 750 Hz, and 1 050 Hz. The PSDs of under-ice ambient noise are calculated using the "pwelch" function in MATLAB software with default Hamming window and 50 000 (equals to the sampling frequency) point FFT length, yielding 1 Hz frequency bins with 50% overlap. It can be seen that the PSDs fluctuate a lot before 06:42, are much stable from 06:42 to 11:42, increase slowly from 11:42 to 15:42, and increase rapidly during the period when the ice canopy was active. Figure 8b shows the Pearson correlation coefficients between the PSDs of under-ice ambient noise at different frequencies and meteorological variables. In this paper, we limit the maximum frequency to 3 kHz as previous works (Milne and Ganton, 1964; Ganton and Milne, 1965; Urick, 1984) have demonstrated that the frequency of thermally induced and wind induced under-ice ambient noise mainly focus in the low-frequency. It can be seen that the PSDs of under-ice ambient noise show higher correlation with the atmosphere temperature especially when the frequency is lower than 2 kHz (Pearson correlation coefficients>0.5). However, the Pearson correlation coefficients fluctuate a lot when the frequency is greater than 2 kHz. One can also find that the PSDs show weak correlation with the wind speed (Pearson correlation coefficients at most frequency are smaller than 0.3). This result is reasonable because the wind cannot induce ocean waves in the experimental area due to the almost fully covered ice canopy. Therefore, wind cannot directly cause changes in the under-ice ambient noise. However, atmosphere temperature variations can cause direct influence to the ice canopy such as melting and breaking, making the under-ice ambient noise change.

4 Conclusions

In this paper, under-ice ambient noise recorded at the long-term ice station during the 9th Chinese National Arctic Research Expedition is studied. Sea ice-induced impulsive noises (ice collision and ice breaking noise) are firstly analyzed using two 7-s-long noise samples. Both noises show obvious impulsive characteristic and their amplitude can be better fitted by sαs distribution. However, the durations of two noises are very different that the ice collision noise lasts for several seconds while the duration of ice breaking noise is much shorter (i.e., less than tens of milliseconds). Using the limited meteorological variables, we deduce that the impulsive ambient noise was caused by the combination of high wind speed and increasing atmosphere temperature on the ice canopy. The Pearson correlation coefficients between long-term PSD variations of under-ice ambient noise and meteorological variables indicate that the under-ice ambient noise was more correlated with the atmosphere temperature (especially the low frequency) compared with wind speed. Other met-

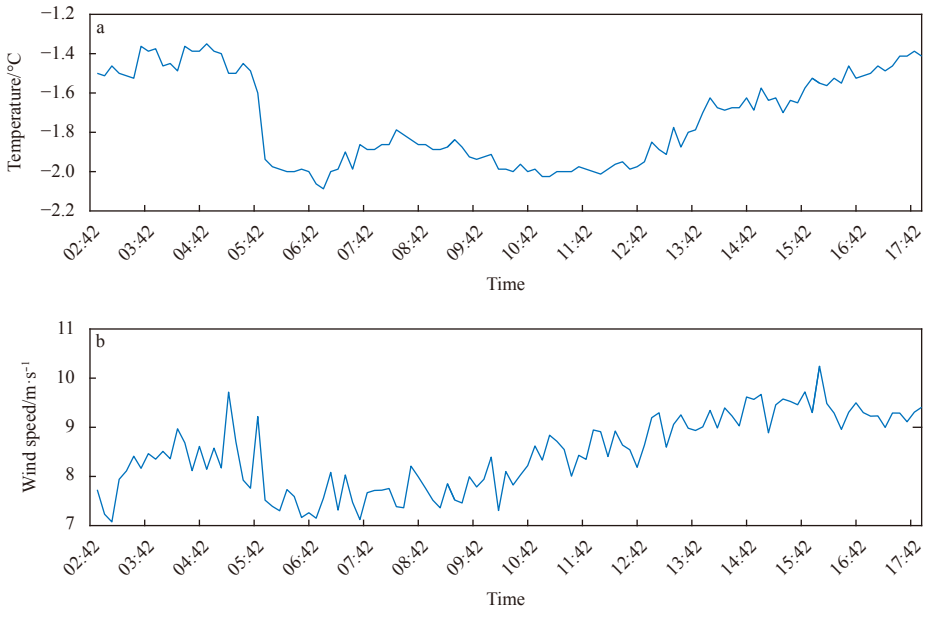

Fig. 7. Atmosphere temperature (a) and wind speed (b) recorded on August 18 by meteorological station on the R/V *Xuelong* from 02:50 to 17:54. Note that the meteorological data are averaged every 8 min corresponding to the length of each signal file.

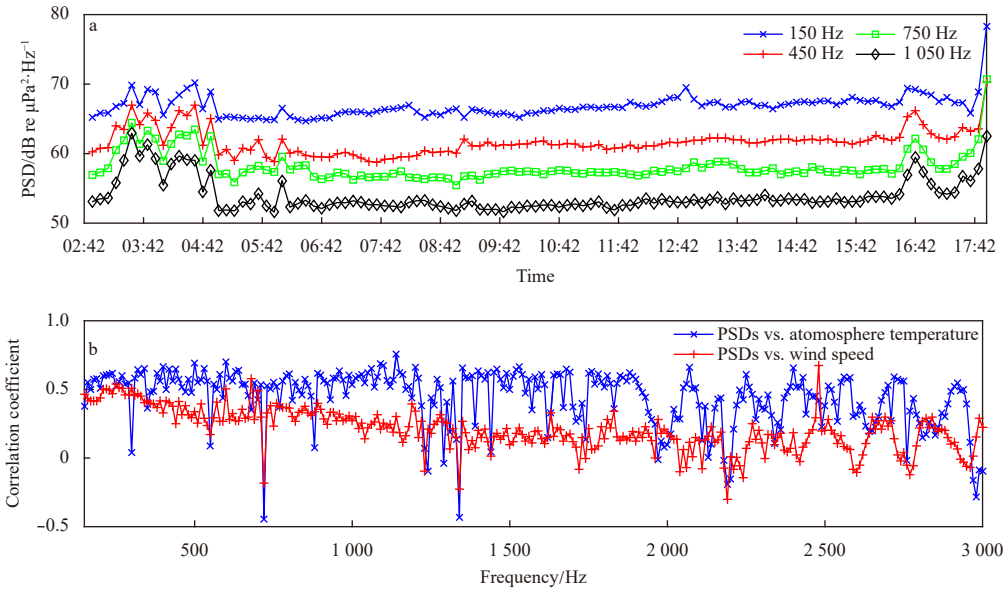

Fig. 8. The PSD variations along with time at different frequencies of under-ice ambient noise (a); and the Pearson correlation coefficients between the PSDs of under-ice ambient noise at different frequencies and meteorological variables (b).

eorological variables such as currents in the upper water column are definitely important contributors to under-ice ambient noise. Therefore, the relationship between under-ice ambient noise in the Arctic Ocean and more meteorological variables will be considered in future work.

Acknowledgement

We thank all participants of the under-ice noise observation experiment of the 9th Chinese National Arctic Research Expedition for their assistance.

References

Audoly C, Gaggero T, Baudin E, et al. 2017. Mitigation of underwater radiated noise related to shipping and its impact on marine life: A practical approach developed in the scope of AQUO project. IEEE Journal of Oceanic Engineering, 42(2): 373–387, doi: 10.1109/JOE.2017.2673938

Bittencourt L, Lima I M S, Andrade L G, et al. 2017. Underwater noise in an impacted environment can affect Guiana dolphin communication. Marine Pollution Bulletin, 114(2): 1130–1134, doi: 10.1016/j.marpolbul.2016.10.037

Brooker A, Humphrey V. 2016. Measurement of radiated underwater noise from a small research vessel in shallow water. Ocean Engineering, 120: 182–189, doi: 10.1016/j.oceaneng.2015.09.048

Carey W M, Evans R B. 2011. Ocean Ambient Noise: Measurement and Theory. New York: Springer, 85–93

Da L L, Wang C, Han M, et al. 2014. Ambient noise spectral properties in the north area of Xisha. Acta Oceanologica Sinica, 33(12): 206–211, doi: 10.1007/s13131-014-0569-4

Deane G B, Glowacki O, Tegowski J, et al. 2014. Directionality of the ambient noise field in an Arctic, glacial bay. The Journal of the Acoustical Society of America, 136(5): EL350–EL356, doi: 10.1121/1.4897354

Ganton J H, Milne A R. 1965. Temperature- and wind-dependent ambient noise under midwinter pack ice. The Journal of the Acoustical Society of America, 38(3): 406–411, doi: 10.1121/1.1909697

Greening M V, Zakarauskas P. 1994. Spatial and source level distributions of ice cracking in the Arctic Ocean. The Journal of the Acoustical Society of America, 95(2): 783–790, doi: 10.1121/1.408388

Huang R K, Zheng H, Kuruoglu E E. 2013. Time-varying ARMA stable process estimation using sequential Monte Carlo. Signal, Image and Video Processing, 7(5): 951–958, doi: 10.1007/s11760-011-0285-x

Johannessen O M, Sagen H, Sandven S, et al. 2003. Hotspots in ambient noise caused by ice-edge eddies in the Greenland and Barents Seas. IEEE Journal of Oceanic Engineering, 28(2): 212–228, doi: 10.1109/JOE.2003.812497

Kinda G B, Simard Y, Gervaise C, et al. 2013. Under-ice ambient noise in Eastern Beaufort Sea, Canadian Arctic, and its relation to environmental forcing. The Journal of the Acoustical Society of America, 134(1): 77–87, doi: 10.1121/1.4808330

Kinda G B, Simard Y, Gervaise C, et al. 2015. Arctic underwater noise transients from sea ice deformation: Characteristics, annual time series, and forcing in Beaufort Sea. The Journal of the Acoustical Society of America, 138(4): 2034–2045, doi: 10.1121/1.4929491

Lewis J K. 1994. Relating Arctic ambient noise to thermally induced fracturing of the ice pack. The Journal of the Acoustical Society of America, 95(3): 1378–1385, doi: 10.1121/1.408576

Lewis J K, Denner W W. 1987. Arctic ambient noise in the Beaufort Sea: Seasonal space and time scales. The Journal of the Acoustical Society of America, 82(3): 988–997, doi: 10.1121/1.395299

Lewis J K, Denner W W. 1988a. Arctic ambient noise in the Beaufort Sea: Seasonal relationships to sea ice kinematics. The Journal of the Acoustical Society of America, 83(2): 549–565, doi: 10.1121/1.396149

Lewis J K, Denner W W. 1988b. Higher frequency ambient noise in the Arctic Ocean. The Journal of the Acoustical Society of America, 84(4): 1444–1455, doi: 10.1121/1.396591

Lin J H, Jiang G J, Gao W, et al. 2005. Measurements and analyses of the vertical distribution of ocean ambient noise. Haiyang Xuebao (in Chinese), 27(3): 32–38

Makris N C, Dyer I. 1986. Environmental correlates of pack ice noise. The Journal of the Acoustical Society of America, 79(5): 1434–1440, doi: 10.1121/1.393671

Makris N C, Dyer I. 1991. Environmental correlates of Arctic ice-edge noise. The Journal of the Acoustical Society of America, 90(6): 3288–3298, doi: 10.1121/1.401439

McCulloch J H. 1986. Simple consistent estimators of stable distribution parameters. Communications in Statistics-Simulation and Computation, 15(4): 1109–1136, doi: 10.1080/03610918608812563

Milne A R, Ganton J H. 1964. Ambient noise under Arctic sea ice. The

Journal of the Acoustical Society of America, 36(5): 855–863, doi: 10.1121/1.1919103

Ozanich E, Gerstoft P, Worcester P F, et al. 2017. Eastern Arctic ambient noise on a drifting vertical array. The Journal of the Acoustical Society of America, 142(4): 1997–2006

Pritchard R S. 1984. Arctic Ocean background noise caused by ridging of sea ice. The Journal of the Acoustical Society of America, 75(2): 419–427, doi: 10.1121/1.390465

Roth E H, Hildebrand J A, Wiggins S M, et al. 2012. Underwater ambient noise on the Chukchi Sea continental slope from 2006–2009. The Journal of the Acoustical Society of America, 131(1): 104–110, doi: 10.1121/1.3664096

Shen X R, Zhang H, Xu Y, et al. 2016. Observation of alpha-stable noise in the laser gyroscope data. IEEE Sensors Journal, 16(7): 1998–2003, doi: 10.1109/JSEN.2015.2506120

Stoyanov S V, Samorodnitsky G, Rachev S, et al. 2006. Computing the portfolio conditional value-at-risk in the alpha-stable case. Probability and Mathematical Statistics, 26(1): 1–22

Urick R J. 1984. Ambient Noise in the Sea. Washington, DC: Undersea Warfare Technology Office, Naval Sea System Command, Department of the Navy, 3–21

Yang Q L, Yang K D, Duan S L. 2018. A method for noise source levels inversion with underwater ambient noise generated by typhoon in Deep Ocean. Journal of Theoretical and Computational Acoustics, 26(2): 1850007, doi: 10.1142/S259172851850007X